NASA TECHNICAL NOTE

NASA TN D-3746

NASA TN D-3746

GPO PRICE $ _____

CFSTI PRICE(S) $ 1.00

Hard copy (HC) _____

Microfiche (MF) 150

ff 653 July 65

FACILITY FORM 602

N67 11958 (ACCESSION NUMBER) (THRU)

18 (PAGES) 1 (CODE)

(NASA CR OR TMX OR AD NUMBER) 12 (CATEGORY)

EXPERIMENTAL INVESTIGATION OF LIQUID OUTFLOW FROM CYLINDRICAL TANKS DURING WEIGHTLESSNESS

by Joseph D. Derdul, Lynn S. Grubb, and Donald A. Petrash

Lewis Research Center
Cleveland, Ohio

NATIONAL AERONAUTICS AND SPACE ADMINISTRATION • WASHINGTON, D. C. • DECEMBER 1966

NASA TN D-3746

EXPERIMENTAL INVESTIGATION OF LIQUID OUTFLOW FROM CYLINDRICAL TANKS DURING WEIGHTLESSNESS

By Joseph D. Derdul, Lynn S. Grubb, and Donald A. Petrash

Lewis Research Center
Cleveland, Ohio

NATIONAL AERONAUTICS AND SPACE ADMINISTRATION

For sale by the Clearinghouse for Federal Scientific and Technical Information
Springfield, Virginia 22151 – Price $1.00

EXPERIMENTAL INVESTIGATION OF LIQUID OUTFLOW FROM CYLINDRICAL TANKS DURING WEIGHTLESSNESS

by Joseph D. Derdul, Lynn S. Grubb, and Donald A. Petrash

Lewis Research Center

SUMMARY

As part of a study of the behavior of rocket engine propellants in space vehicle tanks exposed to weightlessness, an investigation was conducted to determine the behavior of the liquid-vapor interface during outflow from a cylindrical container.

The distortion of the interface, expressed as a dimensionless distortion parameter, was correlated with the Weber number (ratio of pressure to capillary forces) with initial filling as a parameter. The distortion parameter was an approximate measure of the fraction of liquid remaining on the tank walls during outflow, and was therefore related to the total amount of liquid remaining in the tank at the time of vapor ingestion into the outlet. The distortion parameter increased as the Weber number increased to a value of approximately 2, and appeared to remain constant for higher Weber numbers. In general, the distortion parameter increased with lower initial fillings.

Three tank bottom and outlet configurations were included in the study. The shape of the tank bottom and the position of the outlet had essentially no effect on the distortion parameter.

INTRODUCTION

As part of a study of the behavior of rocket engine propellants in space vehicle tanks exposed to weightlessness (zero gravity), an investigation was conducted to determine the effect of outflow on the distortion of the liquid-vapor interface in a weightless environment.

A large portion of the zero-gravity research work has been to determine a means of assuring that liquid is located over the pump inlet prior to engine starting (refs. 1 to 4). Comparatively little work has been devoted, however, to studying the effect of liquid outflow on the behavior of the liquid-vapor interface. Fairbrother and Stubbs (ref. 5)

and Taylor (ref. 6) measured the liquid-volume fraction remaining when liquid was blown from a long capillary tube. Their experiments were conducted at Bond numbers (ratio of acceleration to capillary forces) less than 1, and therefore comparable to those of this study. Although the same algebraic form of the liquid-volume fraction will be used in this report, Taylor's results are not directly applicable because the viscous and inertial forces are of similar magnitude in capillary tubes. In the present investigation, the tank sizes are such that the viscous forces are negligible. A photographic study of outflow from cylindrical tanks during weightlessness (ref. 7) indicated that baffling of the incoming pressurization gas to avoid direct impingement on the interface and of the outlet to retard vapor ingestion can minimize interface distortion and maximize the total amount of liquid removed from the tanks.

This report presents the results of a quantitative experimental investigation of the behavior of the liquid-vapor interface in cylindrical tanks during liquid outflow in a weightless environment. The results indicate that, while distortion of the interface does occur during outflow, significant quantities of liquid can be removed from the tank before vapor enters the outlet line. A Weber number criterion (consisting essentially of the ratio of pressure to capillary forces) was useful in correlating the magnitude of the interface distortion. This investigation was conducted in a 2.25-second drop tower facility over a range of tank sizes, tank bottom configurations, and liquid properties.

SYMBOLS

A_o cross-sectional area of outlet, cm^2

A_t cross-sectional area of tank, cm^2

F_c capillary forces, dynes

F_p pressure forces, dynes

R cylinder radius, cm

V liquid-vapor interface velocity at centerline of tank in weightlessness, cm/sec

V_m mean liquid velocity in weightlessness, $A_o V_o / A_t$, cm/sec

V_o outlet velocity in weightlessness, cm/sec

We Weber number, $We = \rho V_m^2 R / 4\sigma$

ρ liquid density, g/cm^3

σ surface tension, dynes/cm

APPARATUS

Test Facility

The experimental investigation was conducted in the Lewis zero-gravity research facility shown schematically in figure 1. This facility provides 2.25 seconds of unguided free fall. The experiment is recovered by allowing the package to impact in a bed of sand. A high weight-to-frontal area drag shield, balanced about its vertical geometric axis, completely enclosed the experiment package during the drop and thereby minimized air drag on the test package. Thus, the facility was capable of providing the experiment with an acceleration environment of less than 10^{-5} g.

Experiment Package

The experiment package (fig. 2) consisted of a framework for mounting and illuminating the experiment tank and a 16-millimeter high-speed camera, operating nominally at 500 frames per second, for photographing the interface during outflow. Auxiliary equipment on board included a solenoid-operated air piston which acted as an outlet valve for the tank, a pressure supply system, rechargeable nickel-cadmium batteries, and the necessary electrical controls.

Experiment Tanks

Schematic drawings of the tank bottoms and outlet configurations are shown in figure 3. The tanks were cylinders machined from cast acrylic plastic and were 1, 2, 4, and 8 centimeters in radius R. A 0.5-centimeter-radius flat-bottom tank was constructed from borosilicate glass tubing.

As discussed in reference 7, an inlet baffle minimizes the distortion of the interface during outflow in weightlessness. Accordingly, an inlet air deflector plate, equal in diameter to the tank radius and placed one-half radius below the inlet, was used in each case.

The outlets of the tanks were square-edged and located as shown in figure 3. The ratio of tank to outlet radii was 10 in all cases except in the 2-centimeter-radius tanks shown in figures 3(a) and (b) where a ratio of 5 was also used. The outlet tube length in all instances was equal to five times its inside diameter.

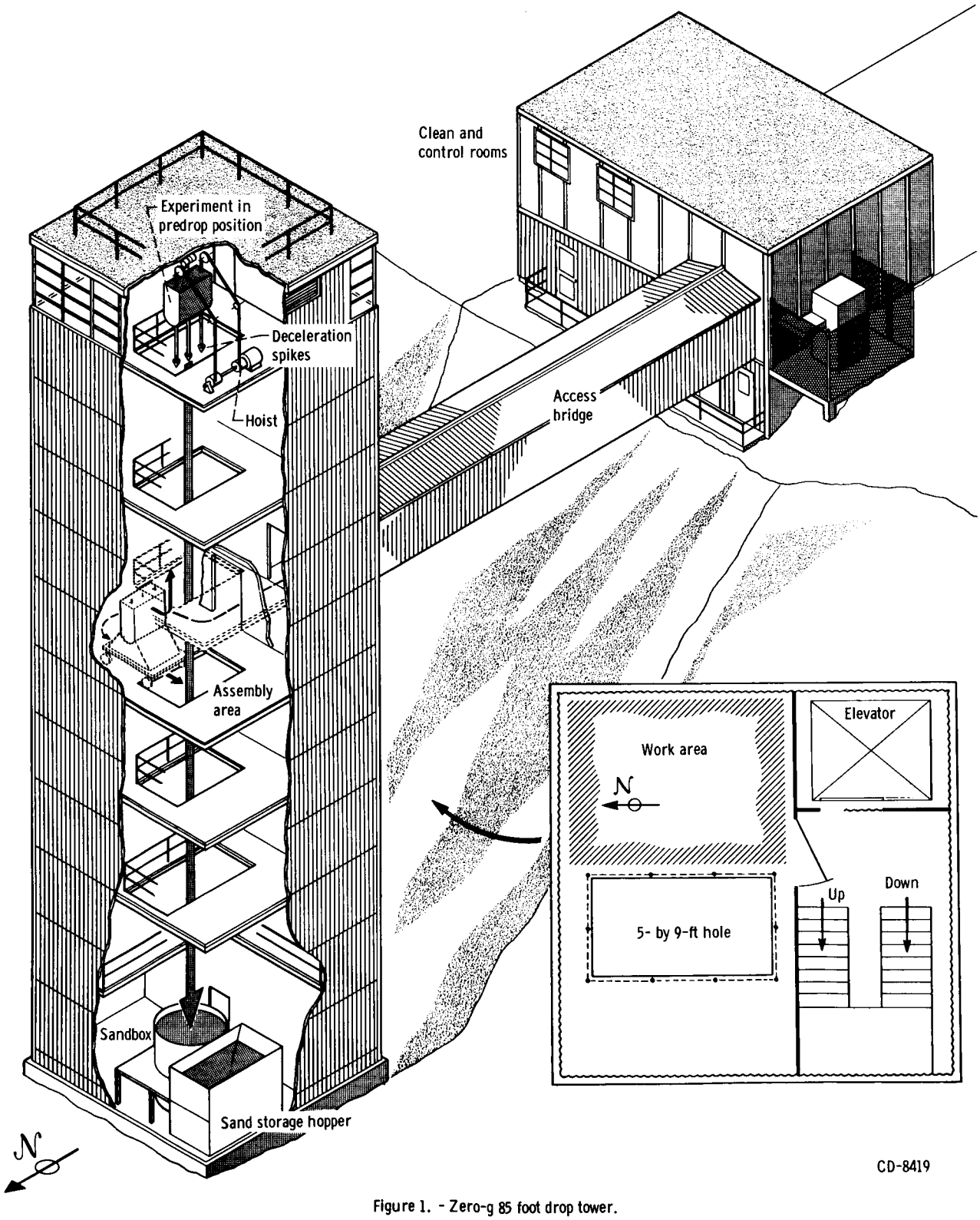

Figure 1. - Zero-g 85 foot drop tower.

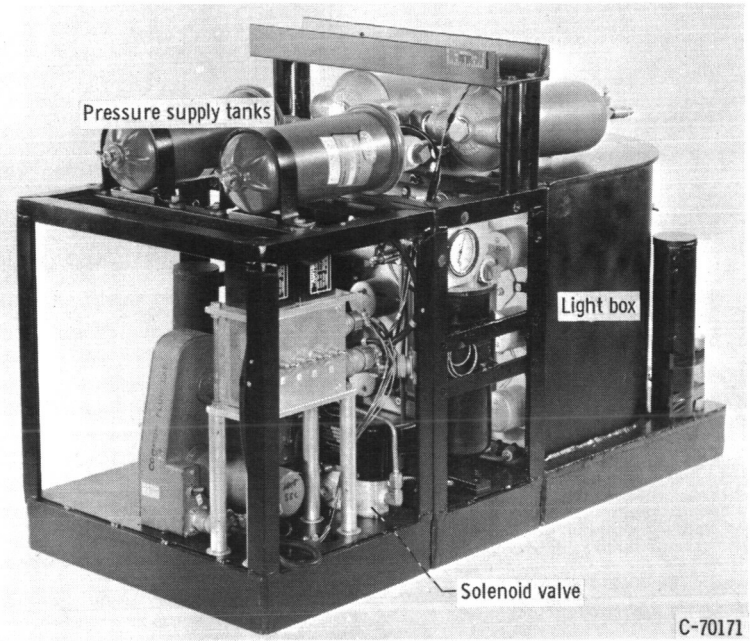

(a) Components.

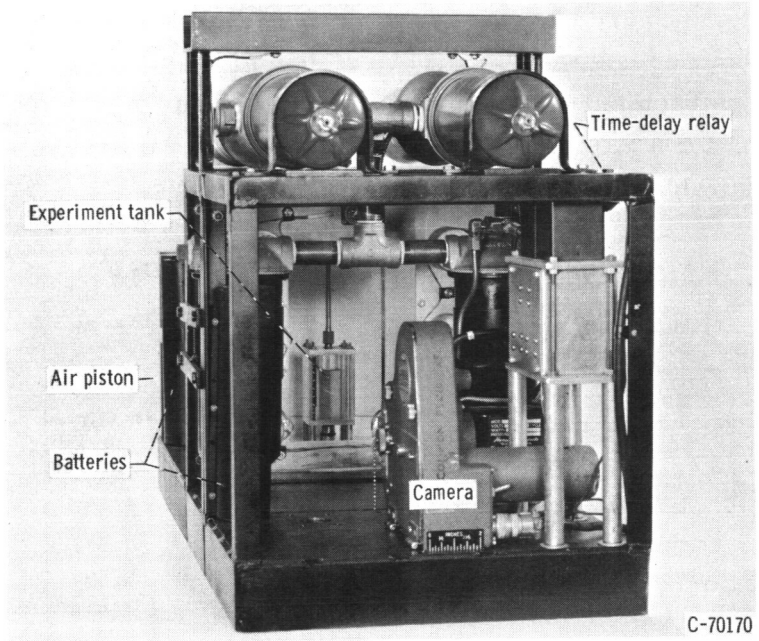

(b) Mounted tank.

Figure 2. - Experiment package.

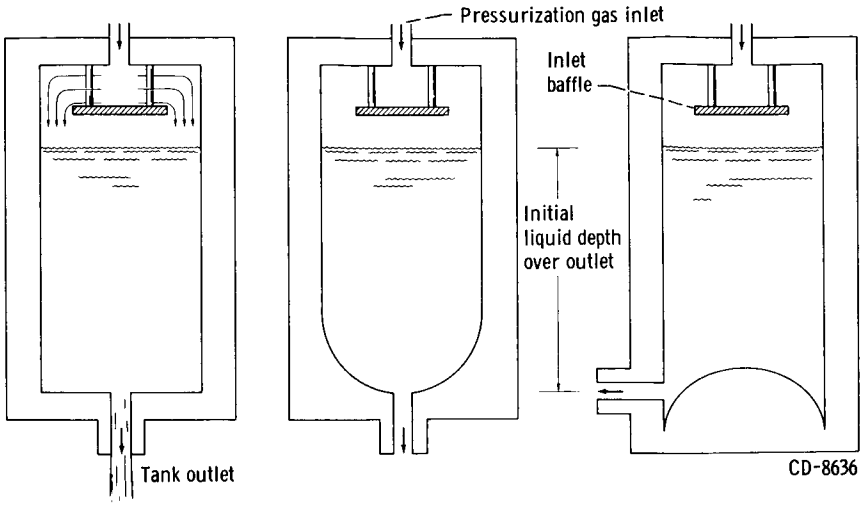

(a) Flat bottom. (b) Hemispherical bottom. (c) 55° Elliptical bottom.

Figure 3. - Schematic drawings of tank geometries.

Test Liquids

The pertinent physical properties of the liquids used in this investigation are listed in table I. These liquids were chosen to have surface tension to density ratios similar to most rocket propellants in use today. Likewise, the 0^{o} contact angle of propellants on tankage materials has been preserved in this study. To improve the photographic quality of the liquids, a small quantity of dye was added to each of the liquids. The addition of the dye had no measurable effect on these physical properties.

TABLE I. - PROPERTIES OF TEST LIQUIDS

[Contact angle of liquid to solid phase (acrylic plastic or borosilicate glass), 0^{o}.]

Liquid	Viscosity, cP	Surface tension, dynes/cm	Density, g/cm^3
Trichlorotrifluoroethane	0.7	18.6	1.579
Carbon tetrachloride	.969	26.9	1.594
1,1,1 Trichloroethane	.865	26.2	1.323
60 Anhydrous ethanol + 40 glycerol, percent by volume	15.4	26.9	.988
Anhydrous ethanol	1.2	22.3	.789
Anhydrous methanol	.597	22.6	.793

Operating Procedure

A typical model tank is shown mounted in the experiment package in figure 2(b). Prior to a series of test runs, the tank and all equipment which contacted the liquid were cleaned in an ultrasonic cleaner with a mild aqueous detergent solution, rinsed with distilled water, and dried with warm filtered air. The tank was assembled in a clean room and then mounted in the experiment package. Finally, the package was balanced about its vertical geometric axis.

Two runs were made at the same pressure for each data point. A normal-gravity run was made to determine the outlet velocity and a weightless run to determine the interface velocity. For each, the tank was filled to the desired level above the outlet, sealed, pressurized, and checked for leaks. Outflow was initiated by opening the tank outlet valve, and the resulting interface motion was recorded by the camera.

The weightless run incorporated a time delay before the initiation of outflow to allow the interface to partially assume its zero-gravity configuration. Upon entering weightlessness, the interface begins a damped oscillation about its zero-gravity equilibrium configuration, which, for a liquid-solid system of 0^{o} contact angle, is a hemisphere equal in radius to that of the tank. An attempt was made to commence outflow at the lowest point of the first oscillation.

Data Reduction

All data were taken from 16-millimeter motion-picture film. To measure distance a millimeter scale was attached outside the experiment tank. By placing an identical scale inside the tank and comparing the two, corrections were made for errors due to light refraction and parallax. Time during the run was recorded either by a digital clock placed in the field of view, or by a known frequency timing trace applied to the edge of the film.

For a given pressure, the centerline interface velocity V under weightless conditions was obtained by measuring the slope of a time-displacement curve of the interface motion. When the outlet velocity from a normal-gravity run at the same pressure was used, the outlet velocity V_o in weightlessness was obtained by subtracting the velocity increment due to static head. The product of the outlet velocity V_o and the area ratio of outlet to tank A_o/A_t yielded the mean liquid velocity V_m in weightlessness. The mean liquid velocity was varied from 4.54 to 64.7 centimeters per second.

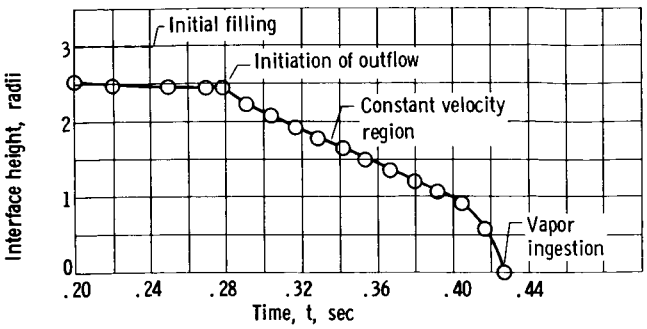

Figure 4. - Typical time-displacement curve of liquid-vapor interface centerline during outflow from a cylindrical tank.

RESULTS AND DISCUSSION

Outflow Characteristics in Cylindrical Tanks 3 Radii Full

The results of a typical outflow test during weightlessness are presented in figure 4 in the form of a time-displacement curve of the motion of the liquid-vapor interface along the tank centerline. Sufficient time is allowed, after placing the system in a weightless environment, for the interface to reach the lowest point in its first oscillation, at which time outflow is initiated. After a short transient period, a constant interface velocity V is reached. This velocity is maintained until the interface approaches the outlet, whereupon ingestion of vapor into the outlet takes place.

In discussing some of the pertinent dimensionless parameters which characterize liquid behavior, Reynolds (ref. 8) suggests that the Weber number, composed essentially of the ratio of pressure (inertia) forces to capillary (surface tension) forces, may be used as an index of the stability of the liquid-vapor interface during flow. For the immediate problem of liquid flow from a cylindrical container of radius R, the Weber number is defined to be

$$We = \frac{F_p}{F_c} = \frac{\frac{1}{2}\rho V_m^2(\pi R^2)}{\sigma(2\pi R)} = \frac{\rho V_m^2 R}{4\sigma}$$

Data obtained in tanks 3 radii full are presented in figure 5, where the Weber number is plotted against $(V - V_m)/V$. Algebraically, $(V - V_m)/V$ is Taylor's liquid-volume fraction which defined the fraction of liquid remaining on the walls when air is forced through a long capillary tube. Because of the relatively low initial fillings used in the present study, however, $(V - V_m)/V$ is not numerically equal to the liquid-volume fraction and is more properly taken to be a measure of the distortion

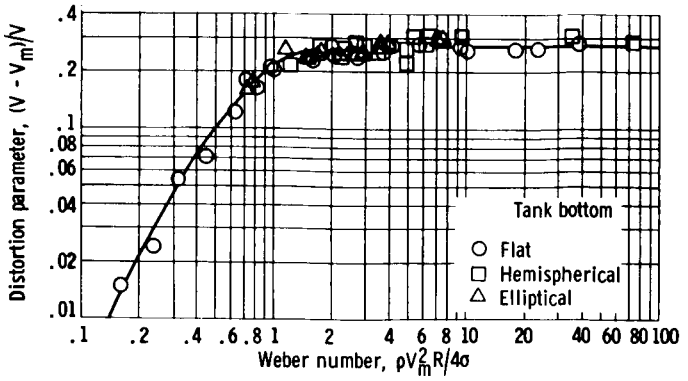

Figure 5. - Effect of outflow on distortion of liquid-vapor interface in cylindrical tanks at initial filling of 3 radii.

of the interface from its normally hemispherical configuration. The distortion parameter may vary from zero (no distortion) to a maximum of one. Figure 5 reveals that as the Weber number increases to approximately 2, the distortion parameter also increases. For Weber numbers greater than 2, the distortion parameter appears to be a constant at about 0.27.

The scatter observed in figure 5 is attributed to the variance of the position of the interface at the beginning of outflow. Upon entering weightlessness, the liquid-vapor interface tends toward the minimum energy configuration consistent with the liquid contact angle. However, since the transition from 1 to 0 g is a step function, residual kinetic energy causes the interface to enter into a damped oscillation about its weightless equilibrium configuration. If the interface was caught at the lowest point of its first oscillation, little if any initial velocity was present. Commencing outflow at any other position results in an initial velocity that may be imparted to the velocity of the interface during outflow. Because of limitations in the experimental apparatus, outflow did not always start at the lowest point as desired.

Effect of tank bottom shape. - Selected photographs (figs. 6 to 8) from tests with the three bottom geometries show the motion of the interface during outflow in weightlessness. The first photograph in each figure shows the interface configuration at 1 g; the remainder of the photographs follow the outflow progress from its inception to vapor ingestion. All three runs were made at nominally the same mean liquid velocity. For those tanks with centrally located outlets, outflow is very similar in nature (figs. 6 and 7). The small wave appearing in figure 6(c) had no effect on the motion of the interface at the centerline and, as a matter of fact, vanishes by figure 6(e). In the tank shown in figure 8, outflow proceeds in much the same manner for approximately 0.15 second. At this point the interface is pulled over to the side and eventually into the outlet because of the streamlines induced by the location of the outlet on the side of the tank. In determining the weightless interface velocity for flow in this geometry, data were considered as long as the axial component of velocity remained constant. Another means of adducing the similarity of flow in all three tank shapes is from the outflow characteristics as presented in figure 5. No parametric spread in the data due to tank shape was observed. As a result, no inherent effect on the bottom geometries was detected until the interface approached the tank outlet; then the influence of the position of the outlet is obvious.

Effect of tank size and ratio of tank to outlet radii. - Three tanks having radii of 1, 2, and 4 centimeters and essentailly the same mean liquid velocity are shown in figure 9. The interface profile in all three cases is similar. All runs shown in figures 6 to 9 were obtained with a ratio of tank to outlet radii of 10. Some data also were obtained with ratios of 5. Data from runs using both ratios are included in figure 5. There appeared to be no parametric spread due to changing the ratio of tank to outlet radii. The outlet apparently

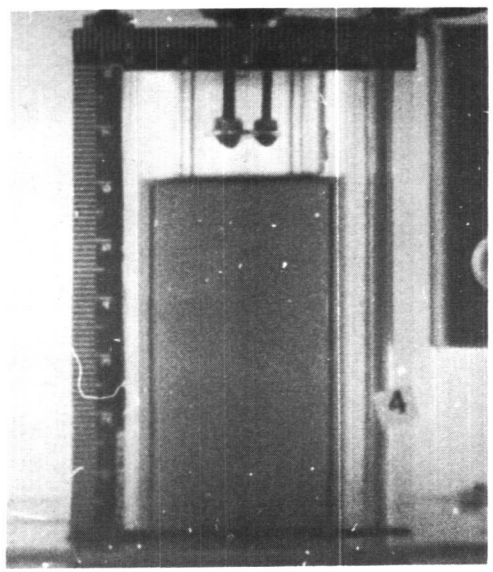

(a) One-g configuration.

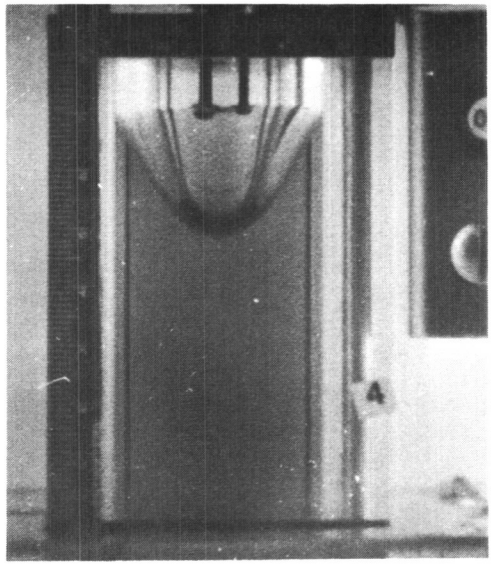

(b) Initiation of outflow; time, 0 second.

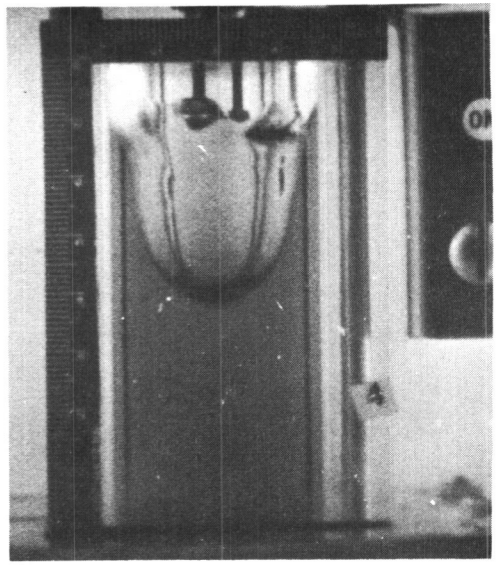

(c) Time, 0.03 second.

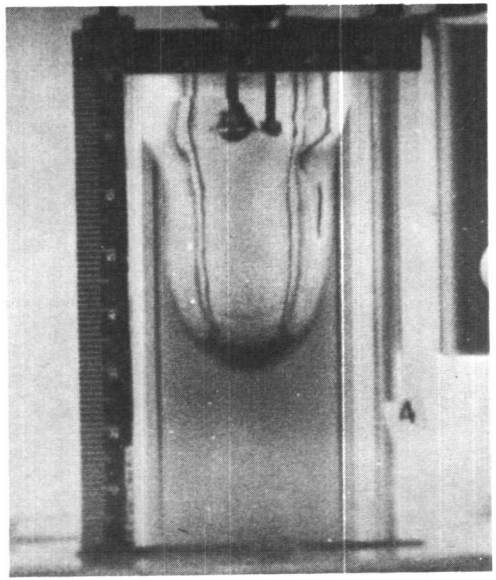

(d) Time, 0.13 second.

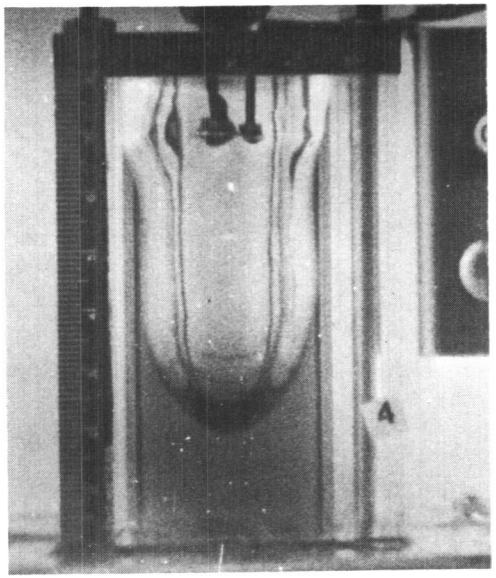

(e) Time, 0.20 second.

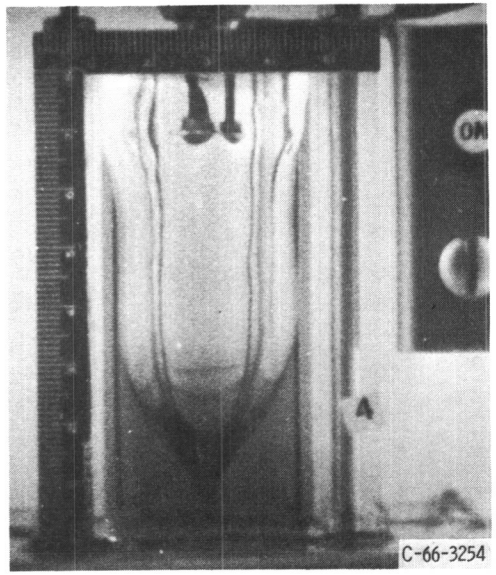

(f) Vapor ingestion; time, 0.25 second.

Figure 6. - Interface configuration during outflow from cylindrical tank with flat bottom in weightlessness. Mean liquid velocity, 10.8 centimeters per second.

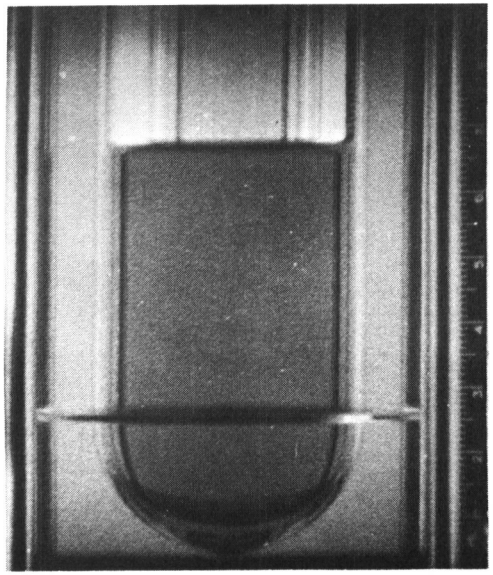

(a) One-g configuration.

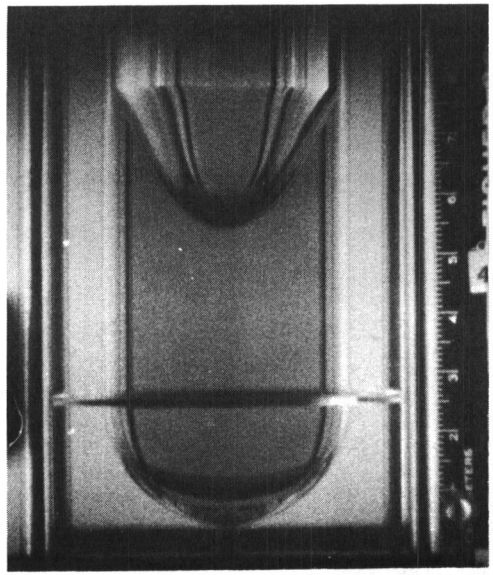

(b) Initiation of outflow; time, 0 second.

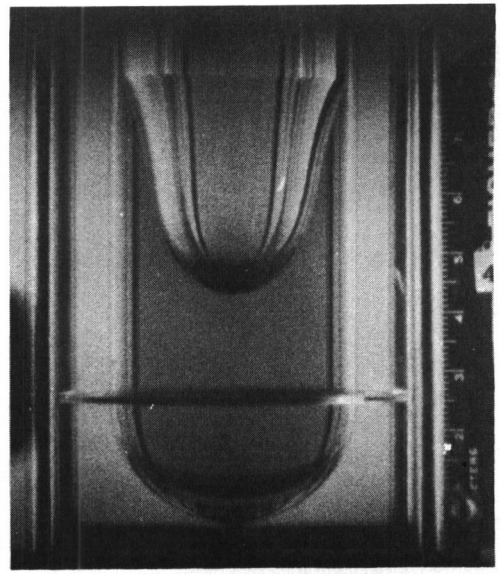

(c) Time, 0.06 second.

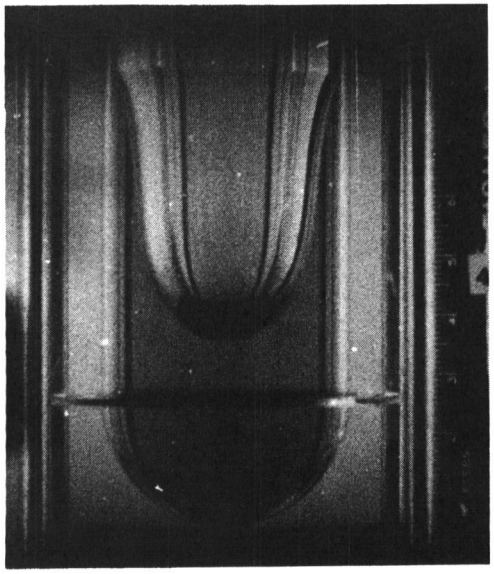

(d) Time, 0.10 second.

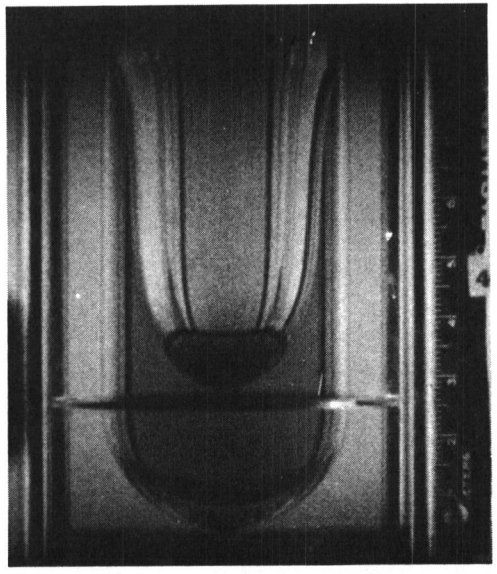

(e) Time, 0.15 second.

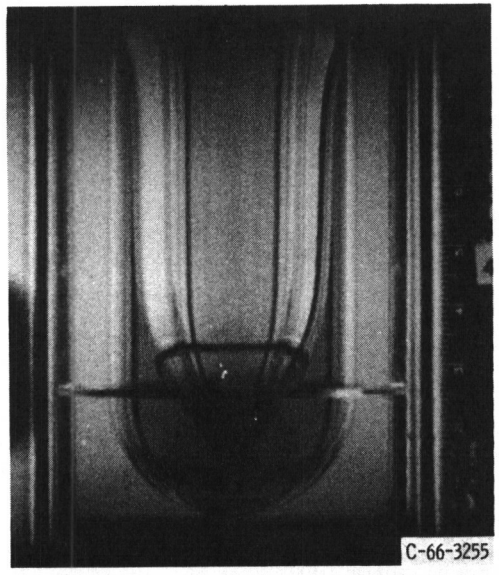

(f) Vapor ingestion; time, 0.22 second.

Figure 7. - Interface configuration during outflow from cylindrical tank with hemispherical bottom in weightlessness. Mean liquid velocity, 11.5 centimeters per second.

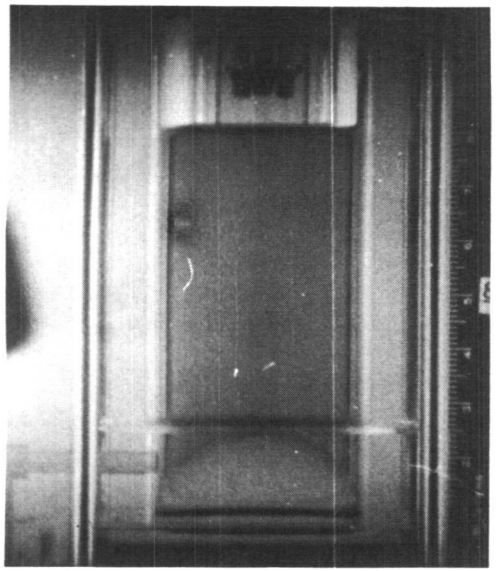

(a) One-g configuration.

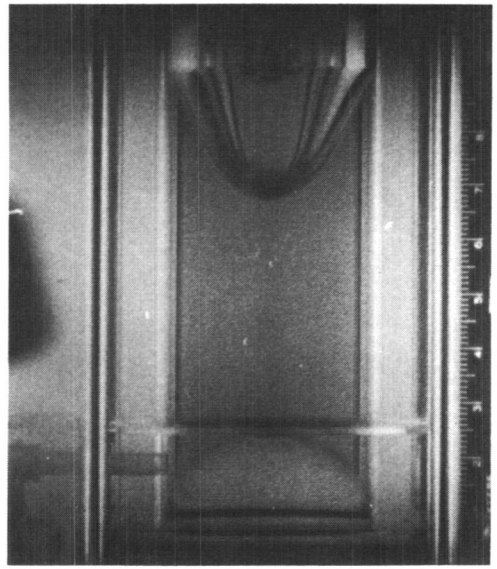

(b) Initiation of outflow; time, 0 second.

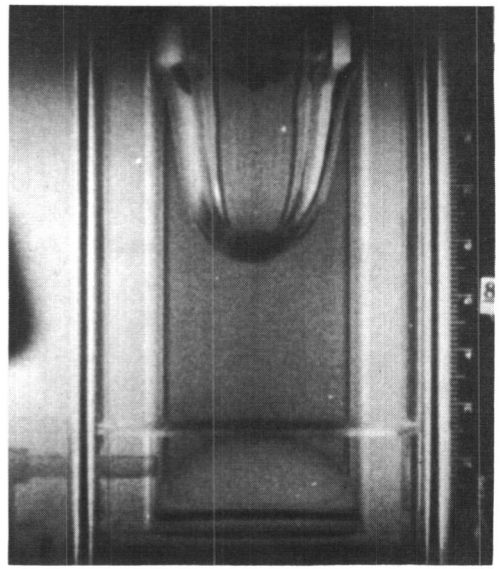

(c) Time, 0.06 second.

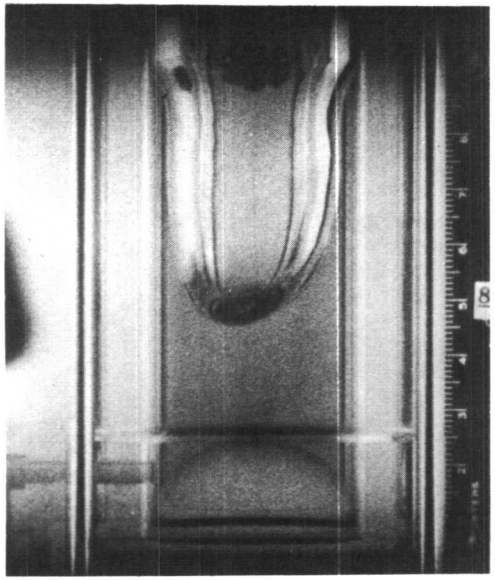

(d) Time, 0.15 second.

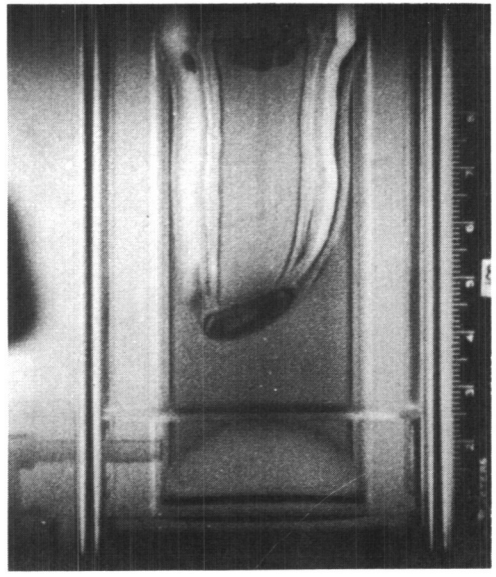

(e) Time, 0.20 second.

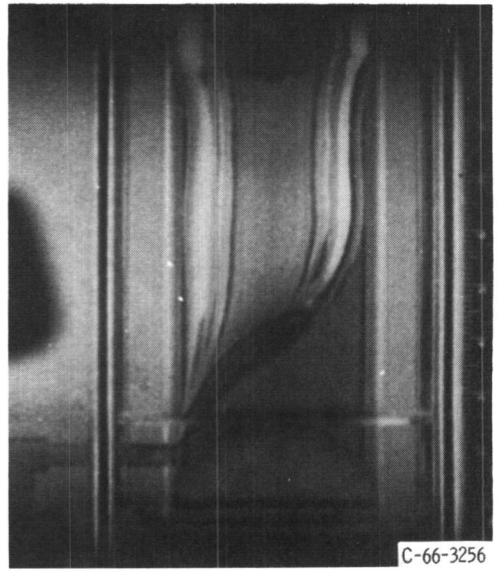

(f) Vapor ingestion; time, 0.26 second.

Figure 8. - Interface configuration during outflow from cylindrical tank with 55° elliptical bottom in weightlessness. Mean liquid velocity, 10.0 centimeters per second.

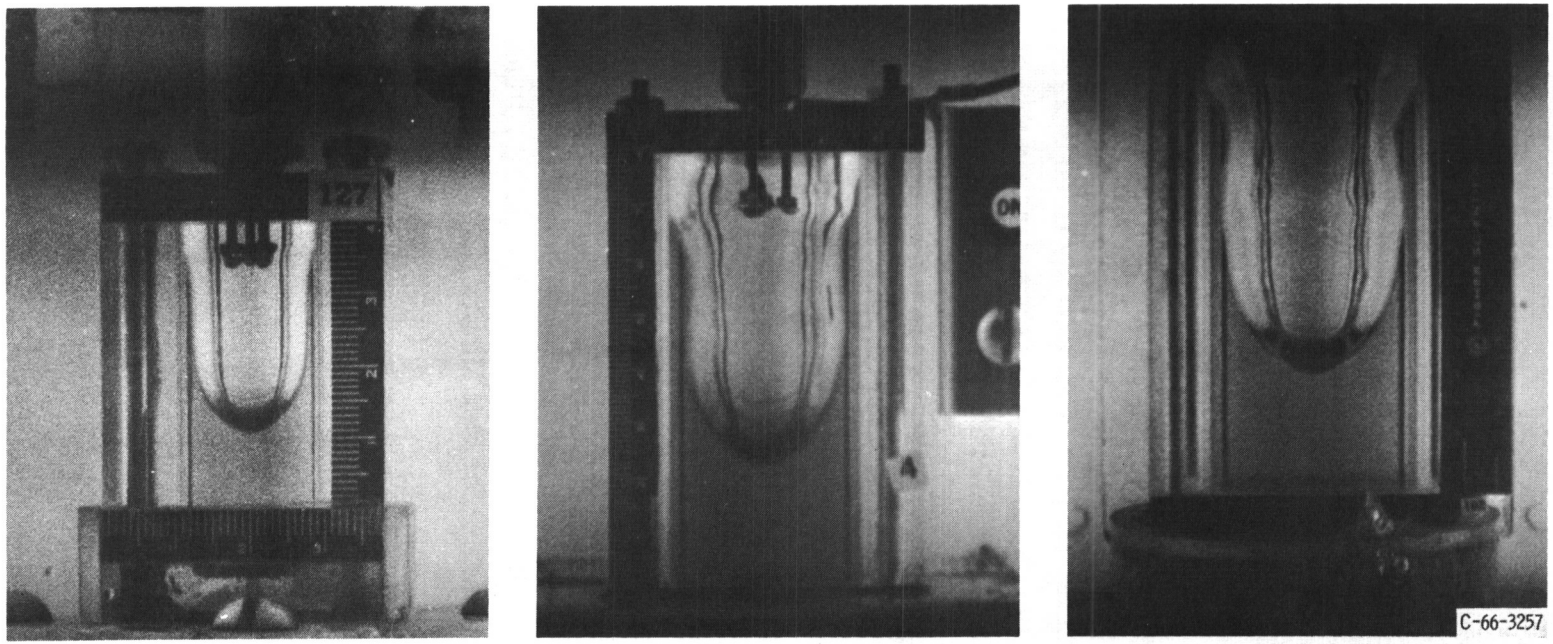

(a) Diameter, 2 centimeters; mean liquid velocity, 10.5 centimeters per second.

(b) Diameter, 4 centimeters; mean liquid velocity, 10.8 centimeters per second.

(c) Diameter, 8 centimeters; mean liquid velocity, 10.2 centimeters per second.

Figure 9. - Effect of tank size on liquid-vapor interface configuration during outflow from cylindrical tank with flat bottom; tank-to-outlet radius ratio, 10.

acted only as an orifice to set the magnitude of the outflow velocity.

Outflow Characteristics as Functions of Initial Filling

The data in the foregoing discussion were obtained with an initial filling of 3 tank radii above the outlet. This filling is representative of relatively full propellant tanks prior to operations such as propellant transfer in orbit. In order to extend the scope of this study, data also were obtained with initial fillings of 2 and 7 radii.

Data runs with initial fillings of 2 and 7 radii were made in a 2-centimeter-radius flat-bottomed cylindrical tank. The distortion parameter $(V - V_m)/V$ for these data is plotted against the Weber number in figure 10. Also presented in figure 10 are the results previously shown in figure 5 for tanks initially filled to a depth of 3 radii. The distortion of the interface in tanks 2 radii full is greater than that obtained in tanks 3 radii full. In tanks initially filled to 7 radii, the distortion of the interface is significantly reduced from that observed at the lower fillings. The scatter observed in the data is a result of the magnitude of the difference between V and V_m, which is so small that it approaches the absolute accuracy of the measurement technique.

In an investigation of this type, it would seem logical to assume that the interface would initially accelerate to some velocity and remain constant until vapor ingestion occurred. Taylor (ref. 6) made this assumption implicitly, and it would seem to be accurate for tanks with very high initial fillings. However, a constant interface velocity results in a constant distortion parameter, which therefore must be independent of initial filling. Since figure 10 clearly shows a dependence on initial filling, the assumption of constant interface velocity is questionable. In fact, the assumption of constant interface velocity, when applied to tanks with relatively low initial fillings, is an oversimplification of the actual phenomenon. The data showed that there were transient regions

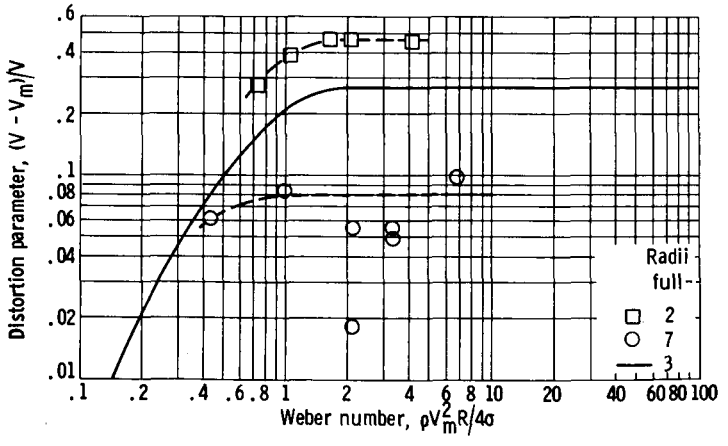

Figure 10. - Effect of initial filling on distortion of liquid-vapor interface during outflow from flat-bottom cylindrical tanks.

both immediately following the inception of outflow and immediately preceding vapor ingestion which were characterized by greatly increased interface distortion (fig. 4). These high-distortion end effects were of relatively minor importance (negligible in Taylor's case) in determining values for the distortion parameter in runs with an initial filling of 7 radii. At lower initial fillings, however, these end effects have a major influence on the outflow pattern, and therefore resulted in higher values of the distortion parameter.

SUMMARY OF RESULTS

An experimental investigation of the behavior of the liquid-vapor interface when subjected to outflow disturbances was conducted in a weightless environment. This investigation, conducted over a range of cylindrical tank sizes and tank bottom shapes and a range of liquids exhibiting 0° contact angles, yielded the following results:

1. The behavior of the liquid-vapor interface, expressed as a distortion parameter, was correlated with the Weber number.
2. The distortion parameter increased as the initial liquid filling decreased.
3. The shape of the bottom of the tank and the position of the outlet had no effect on the distortion parameter.

Lewis Research Center,
National Aeronautics and Space Administration,
Cleveland, Ohio, August 10, 1966,
124-09-03-01-22.

REFERENCES

1. Petrash, Donald A.; Nussle, Ralph C.; and Otto, Edward W.: Effect of Contact Angle and Tank Geometry on the Configuration of the Liquid-Vapor Interface During Weightlessness. NASA TN D-2075, 1963.
2. Petrash, Donald A.; Nelson, Thomas M.; and Otto, Edward W.: Effect of Surface Energy on the Liquid-Vapor Interface Configuration During Weightlessness. NASA TN D-1582, 1963.
3. Masica, William J.; Derdul, Joseph D.; and Petrash, Donald A.: Hydrostatic Stability of the Liquid-Vapor Interface in a Low-Acceleration Field. NASA TN D-2444, 1964.

4. Masica, William J.; and Petrash, Donald A.: Motion of Liquid-Vapor Interface in Response to Imposed Acceleration. NASA TN D-3005, 1965.

5. Fairbrother, Fred; and Stubbs, Alfred E.: Studies in Electro-Endosmosis. Part IV. The "Bubble-Tube" Method of Measurement. Chem. Soc. J., 1935, pp. 527-529.

6. Taylor, G. I.: Deposition of a Viscous Fluid on the Wall of a Tube. J. Fluid Mech., vol. 10, pt. 2, Mar. 1961, pp. 161-165.

7. Nussle, Ralph C.; Derdul, Joseph D.; and Petrash, Donald A.: Photographic Study of Propellant Outflow From a Cylindrical Tank During Weightlessness. NASA TN D-2572, 1965.

8. Reynolds, William C.: Hydrodynamic Considerations for the Design of Systems for Very Low Gravity Environments. Rep. LG-1, Stanford University, Sept. 1, 1961.

NASA-Langley, 1966 E-3434

"The aeronautical and space activities of the United States shall be conducted so as to contribute . . . to the expansion of human knowledge of phenomena in the atmosphere and space. The Administration shall provide for the widest practicable and appropriate dissemination of information concerning its activities and the results thereof."

—NATIONAL AERONAUTICS AND SPACE ACT OF 1958

NASA SCIENTIFIC AND TECHNICAL PUBLICATIONS

TECHNICAL REPORTS: Scientific and technical information considered important, complete, and a lasting contribution to existing knowledge.

TECHNICAL NOTES: Information less broad in scope but nevertheless of importance as a contribution to existing knowledge.

TECHNICAL MEMORANDUMS: Information receiving limited distribution because of preliminary data, security classification, or other reasons.

CONTRACTOR REPORTS: Technical information generated in connection with a NASA contract or grant and released under NASA auspices.

TECHNICAL TRANSLATIONS: Information published in a foreign language considered to merit NASA distribution in English.

TECHNICAL REPRINTS: Information derived from NASA activities and initially published in the form of journal articles.

SPECIAL PUBLICATIONS: Information derived from or of value to NASA activities but not necessarily reporting the results of individual NASA-programmed scientific efforts. Publications include conference proceedings, monographs, data compilations, handbooks, sourcebooks, and special bibliographies.

Details on the availability of these publications may be obtained from:

SCIENTIFIC AND TECHNICAL INFORMATION DIVISION

NATIONAL AERONAUTICS AND SPACE ADMINISTRATION

Washington, D.C. 20546